Research Article GU J Sci, Part A, 11(4): 814-825 (2024) 10.54287/gujsa.1553577

Gazi University
Journal of Science
PART A: ENGINEERING AND INNOVATION
http://dergipark.org.tr/gujsa

Investigation of the Effect of Mechanical Alloying on the Wear Behavior of AA7020/Fe_3O_4/GNP Hybrid Composite Materials

Ufuk TAŞCI[1*]

[1] *Department of Graduate School of Natural and Applied Sciences, Gazi University, Ankara, Türkiye*

Keywords

Mechanical Alloy
Hybrid Composite
Graphene
Fe_3O_4
Tribology Behavior

Abstract

In this study, the mechanical properties of composite/hybrid composites were investigated by reinforcing 10% Fe3O4 and 0.25% nanographene by weight into the AA7020 alloy, which is widely preferred, especially in the defense and aviation industries. The prepared mixture powders were subjected to a mechanical alloying process for 1 and 8 hours in a ball mill with a 1/16 powder-ball ratio to distribute them homogeneously. The mixed hybrid/composite powders were produced in a metal mold using a powder metallurgy hot pressing method at 250 MPa load and 575°C temperature for 60 minutes. The microstructural properties of the test samples were investigatedIn addition, density, microhardness and wear test results were examined in terms of mechanical properties. The hybrid sample with 8h mechanical alloying obtained the highest hardness value (118.5 HV) and the lowest friction coefficient (0.1965 µm).

Cite

Taşçı, U. (2024). Investigation of the Effect of Mechanical Alloying on the Wear Behavior of AA7020/Fe_3O_4/GNP Hybrid Composite Materials. *GU J Sci, Part A, 11*(4), 814-825. doi:10.54287/gujsa.1553577

Author ID (ORCID Number)

0000-0002-8577-443X Ufuk TAŞCI

Article Process

Submission Date 20.09.2024
Revision Date 14.10.2024
Accepted Date 25.10.2024
Published Date 30.12.2024

1. INTRODUCTION

Aluminum and its alloys are widely preferred in defense, aerospace, and aviation fields due to their advantageous properties, including low density, high specific strength, hardness, excellent electrical conductivity, and corrosion resistance (Kumar et al., 2023). In addition, due to their low density, aluminum alloys are used in studies to reduce fuel consumption and CO_2 emissions for automotive applications. 7XXX alloys have low density, excellent specific strength and bending rigidity. For this reason, the 7020 alloy belongs to the Al-Zn-Mg-(Cu) group within the 7XXX series and is preferred in the latest technological aviation, space, automotive and rail system applications (Kumar et al., 2014; Kaya et al., 2022). Despite their high mechanical properties, aluminum alloys exhibit low tribological performance under certain conditions (Sharma et al., 2021; Kumar et al., 2022). In particular, metal matrix composites (MMCs) have been developed and continue to be improved to enhance the weak aspects of these materials for modern technologies (Karakoç et al., 2019).

Current aluminum composite materials are favored due to their low density, durability, and enhanced thermal conductivity. However, despite the advanced properties of MMCs, there remains a need to improve their strength and tribological properties (Jiang et al., 2018; Reddy et al., 2018; Özkan et al., 2022). As highlighted in recent studies, hybrid-reinforced composite materials are being utilized. Oxides and ceramics are commonly used in the production of particle-reinforced composite materials. Typically, ceramic reinforcement particles in micron and nano sizes, such as B_4C, Al_2O_3, Graphene, WS_2, HBN, TiC, Fe_3O_4, and SiC, are employed (Karakoç et al., 2019; Sardar et al., 2020; Zheng et al., 2020; Taşcı et al., 2024).

*Corresponding Author, e-mail: ufuktasci@gazi.edu.tr

Production of metal matrix composite materials typically involves manufacturing methods such as conventional casting, stir casting, infiltration, mechanical alloying, and powder metallurgy (PM). However, hybrid/composite materials produced using casting and infiltration methods face a significant challenge in achieving a homogeneous distribution of reinforcement particles within the matrix. To address this, the initial powders are prepared in ball mixers and produced using the powder metallurgy method (Lakshmikanthan et al., 2022; Taşcı & Bostan, 2022; Srivyas et al., 2023; Michael & John, 2024).

The study aims to investigate the effect of 1-hour and 8-hour milling durations, particularly on the mechanical and wear behavior, to ensure the homogeneous distribution of 10 wt.% Fe_3O_4 and 0.25 wt.% GNP hybrid reinforcements within the AA7020 matrix, produced via the powder metallurgy (PM) method.

2. MATERIAL AND METHOD

2.1. Materials and Methods

This study used AA7020 matrix powders (avg. 75 µm), Fe_3O_4 powders (avg. 40 µm), and high-purity nanographene powders with an average size of 5 nm. Mechanical alloying (MA) was carried out by adding 10 wt% Fe_3O_4 powders and 0.25 wt% nanographene powders to AA7020 alloy using an atmosphere-controlled high-energy ball mixer for 1 and 8 h. The mixer was operated at 300 rpm with a powder-to-ball ratio of 1/16. The schematic drawing of the milling process during the MA process is given in Figure 1.

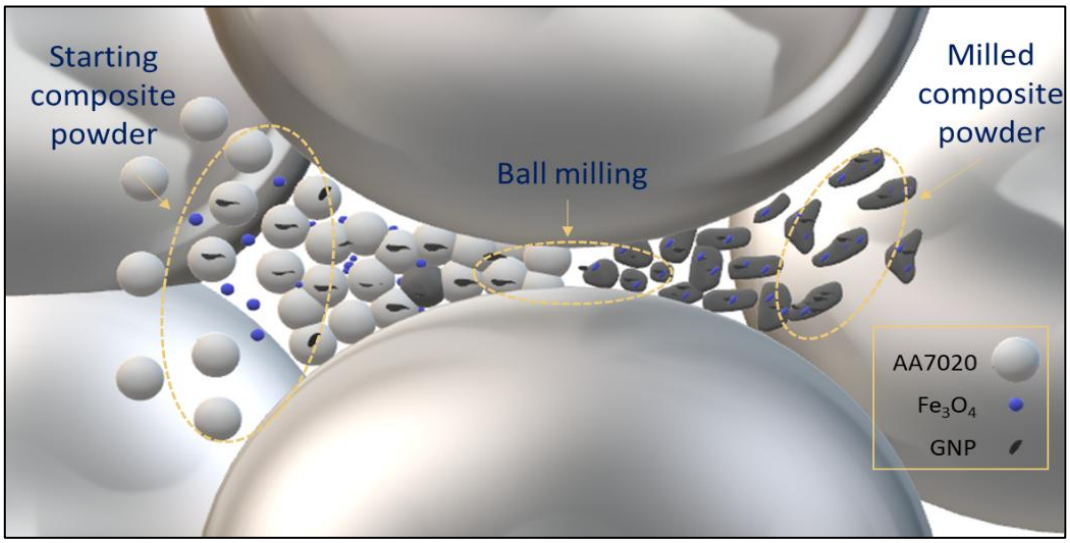

Figure 1. *Preparation of composite powders in ball mill (Taşcı et al., 2024)*

The mixed powders were pressed into 10x10x10 mm^3 cylindrical samples in a powder metal die using the hot pressing method at 575°C and 250 MPa pressure. Table 1 presents the chemical composition of the AA7020 alloy powder material used as the matrix in producing the hybrid composite material.

Table 1*. Chemical composition of AA7020 alloy*

Element	Zn	Mg	Ti	Zr	Fe	Si	Cu	Cr	Mn	Al
Content (%)	4.5	1.40	0.25	0.070	0.4	0.35	0.2	0.10	0.040	Remainder

2.2. Microstructure and Mechanical Analysis

The hybrid composite materials of AA7020+Fe_3O_4+GNP, produced by hot pressing, were sanded in an automatic grinding and polishing machine in a water-based environment using sandpapers of 600, 800, 1000, and 1200 grit, respectively. In sequence, the sanded samples were then polished using diamond suspensions on diamond pads of 9, 6, and 3 microns. Following the polishing process, a final polishing was performed with a 0.001-micron colloidal solution to remove scratches on the sample surface altogether. Lastly, the samples

were etched for 15 seconds using Keller's reagent (1 ml HF + 200 ml H_2O) and examined under an optical microscope. The microstructure images of the samples were captured using a Leica DM4000 M optical microscope.

A scanning electron microscope (SEM) was employed to analyze the morphology of the powders, microstructure images, wear surfaces after wear testing. SEM images, EDS analysis, and mapping of the composites were conducted using a TESCAN MAIA^3 XMU model SEM. Phase analysis was performed using X-ray diffraction (XRD) with a Bruker D_8 Advance X-ray diffractometer.

The hybrid composite materials hardness HV0.5 (ASTM E10-08) and wear (ASTM G99-05) tests (20N load and 1500m wear distance) were conducted in accordance with the relevant standards. Figure 2 presents a schematic diagram of the wear test.

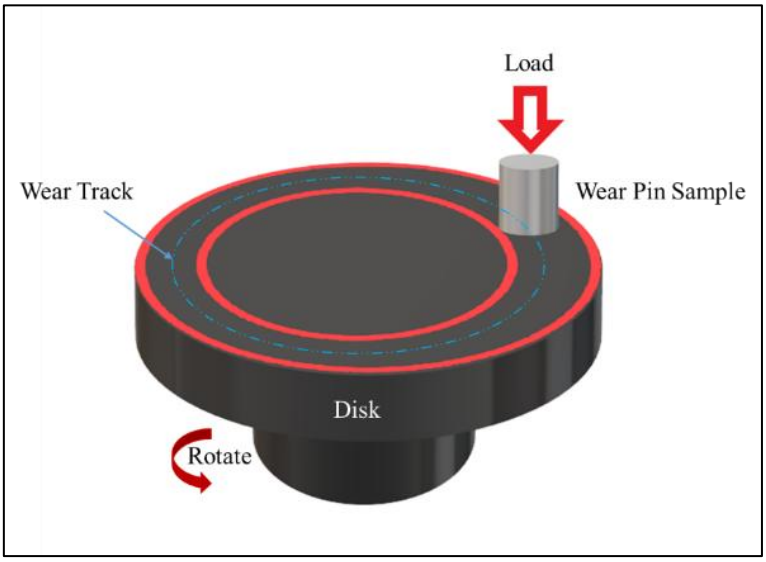

Figure 2. *Wear test setup on composite materials produced in the study (Taşcı et al., 2024)*

3. RESULTS AND DISCUSSION

3.1. Properties of Starting Powder Materials

The SEM images of the AA7020 alloy powder used as the matrix, along with the Fe_3O_4 and GNP reinforcement powders, are presented in Figure 3. The morphology of the AA7020 alloy powder appears spherical, the Fe_3O_4 powder particles exhibit a complex shape, and the GNP shows a two-dimensional lamellar structure.

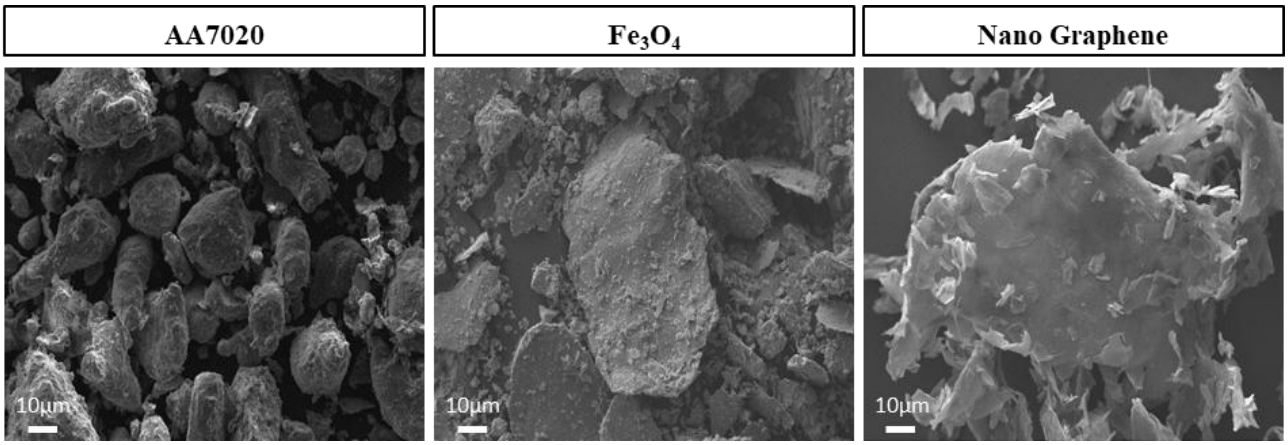

Figure 3. *Images of starting powder materials*

The composite powders' morphology changed significantly from their initial shapes after milling for different durations (1 and 8 hours). SEM analyses, presented in Figure 4, illustrate the effect of the mixing method on the distribution of Fe_3O_4 and GNP reinforcements within the powders. The composite powder, dry-milled with balls, becomes more flattened and adopts a lamellar form compared to the spherical, unreinforced AA7020 powder.

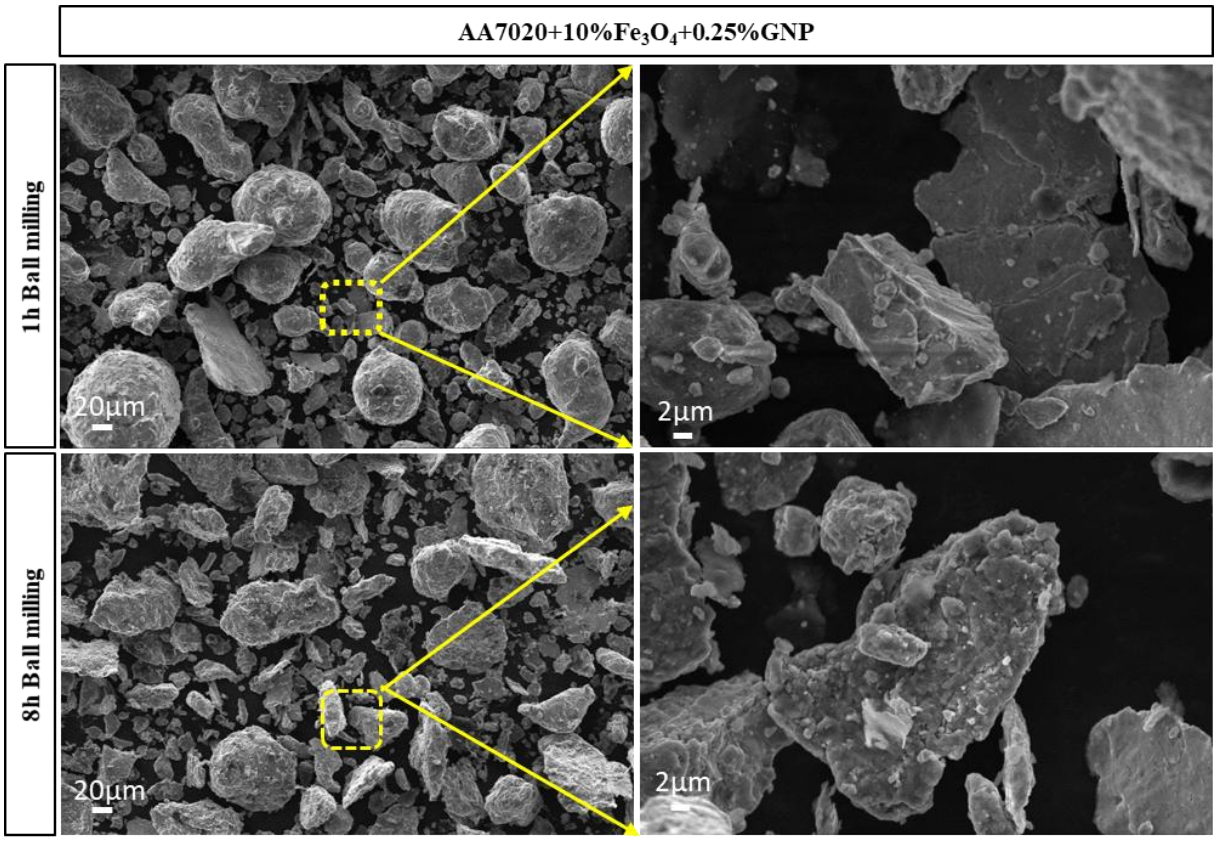

Figure 4. *SEM analysis image of hybrid powders produced by mechanical alloying*

3.2. Microstructural Analysis

The XRD analysis results of the AA7020+10%Fe_3O_4+0.25%GNP hybrid composite material are shown in Figure 5. When the analysis result was examined, it was determined that it contained α-Al matrix phase, Fe_3O_4, GNP, and $AlMg_4Zn_{11}$ intermetallic phase.

In Figure 6, ground hybrid powders were produced by hot pressing at 575°C at 250 MPa pressure in a protective atmosphere. Optical microscope images of the starting matrix AA7020 and hybrid composite AA7020+Fe_3O_4+GNP materials are given.

The homogeneous distribution of reinforcement particles in hybrid composite materials is critical regarding mechanical properties. Figure 6 shows that the agglomeration level in hybrid materials is at low rates due to the mechanical alloying process. Thanks to the ball alloying, AA7020 matrix powders are flattened, and the reinforcement particles are located at the grain boundaries of the matrix powders. Despite being a hybrid reinforcement, the porosity rate is formed at very low levels thanks to mechanical alloying.

Figure 7 shows the microstructure SEM analysis image of the materials. When the images are examined, it is determined that the GNP reinforcement AA7020 matrix powders are significantly flattened due to the 8h grinding process compared to the 1h grinding process. It is thought that with the increase of mechanical alloying time, GNPs flatten the morphology of AA7020 powder without creating cracks with their lubricating properties within the structure. In addition, it was observed that 10% Fe_3O_4 powders by weight were distributed homogeneously in the matrix with increasing alloying time.

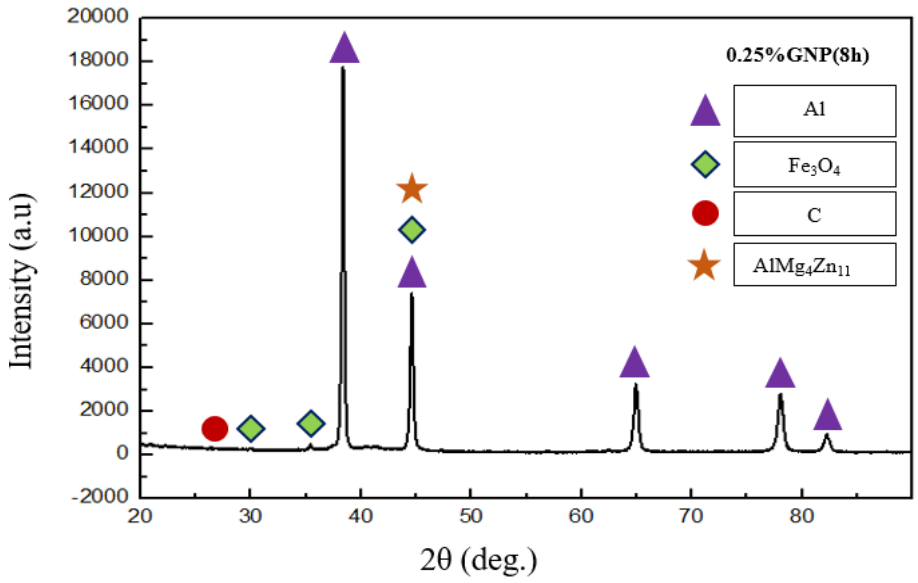

Figure 5. *XRD analysis of AA7020+Fe_3O_4+GNP hybrid composites*

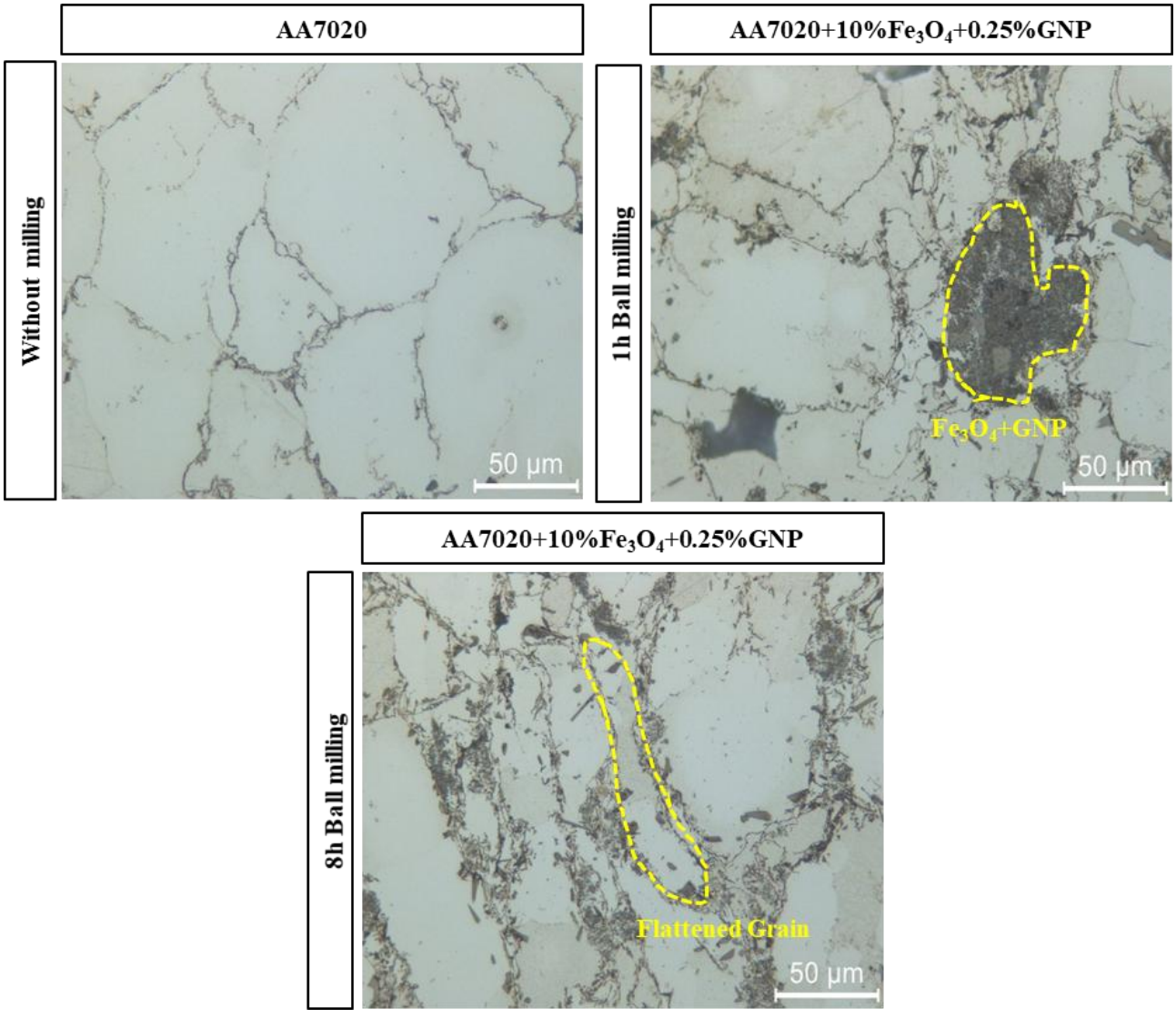

Figure 6. *Optical image of AA7020 alloy and hybrid composite materials*

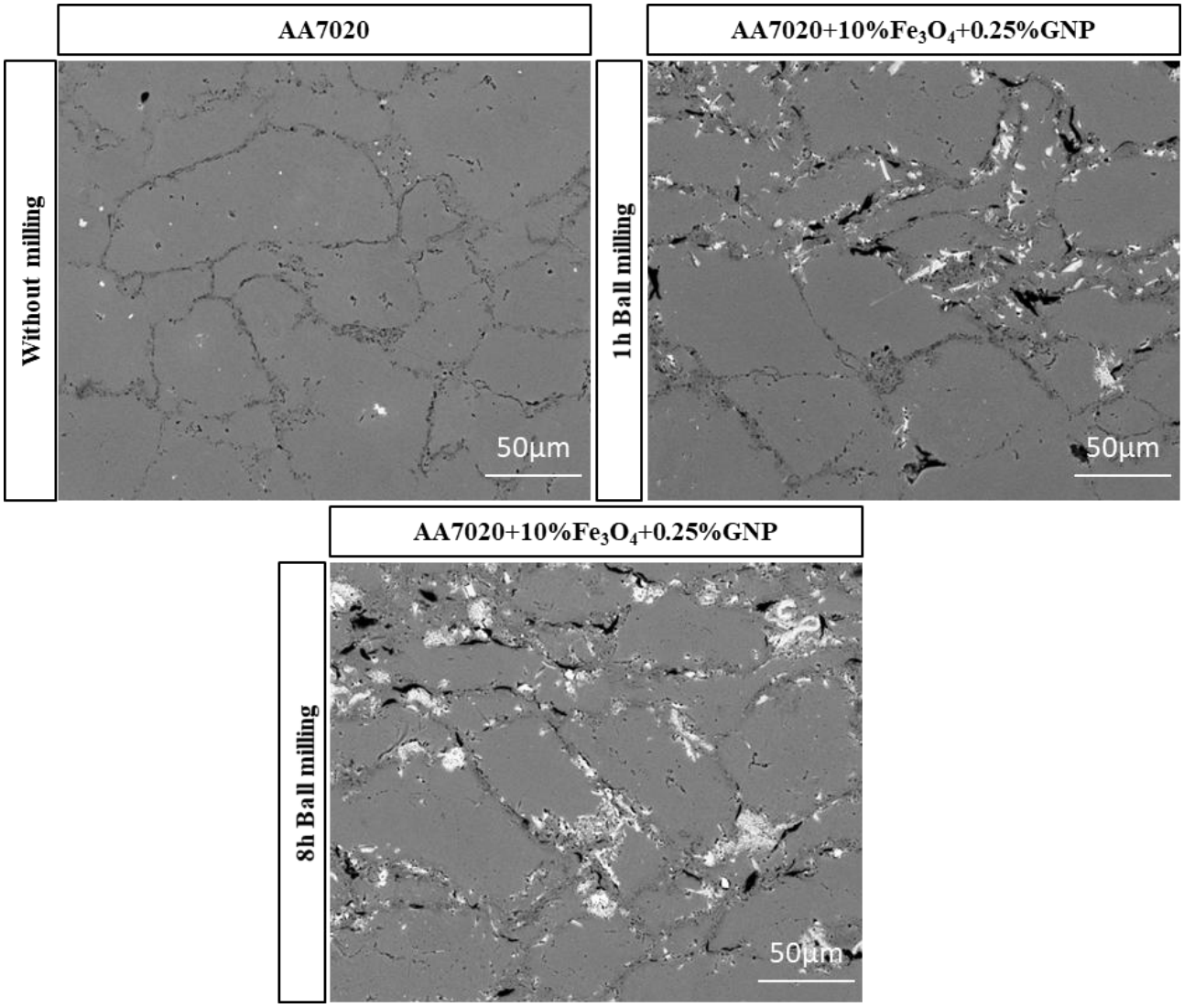

Figure 7. *SEM image of AA7020+10%Fe_3O_4+0.25%GNP hybrid composite material*

3.3. Mechanical Properties

The density and hardness results of the test samples are given in Figure 8. When the graph was examined, the highest density value was 99.3% in the 4h milled hybrid reinforced sample. The lowest density value was determined as 98.8% in the AA7020 sample. When the hardness values are examined, the highest was measured as 118.5 HV in the 8h milled 10%Fe_3O_4+0.25%GNP reinforced sample. The lowest hardness value was determined in the AA7020 alloy without reinforcement and milling process.

3.4. Tribological Behavior

Figure 9 shows the test samples weight loss and specific wear rate (SWR) results. The highest weight loss value was 0.0185 in the AA7020 sample without reinforcement and alloying. The lowest value among the SWR ratios was 4.33* 10^{-7} mm^3/Nm in the hybrid reinforced sample with an 8h grinding process. A similar behavior to the hardness values was observed in the SWR results with increasing grinding hours. This decreases weight loss and SWR values due to increasing hardness values (Kanthavel et al., 2016; Taşcı et al., 2024).

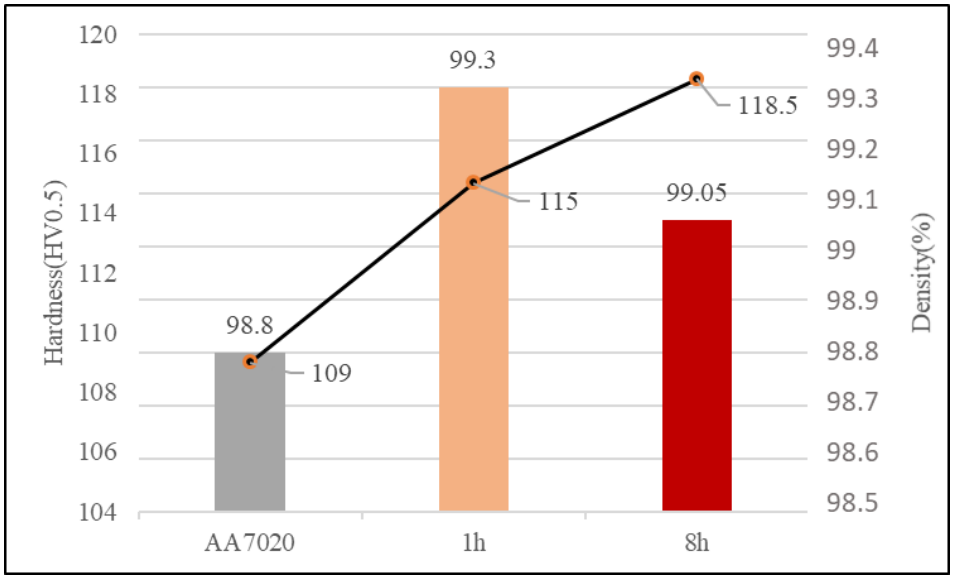

Figure 8. *Density and hardness*

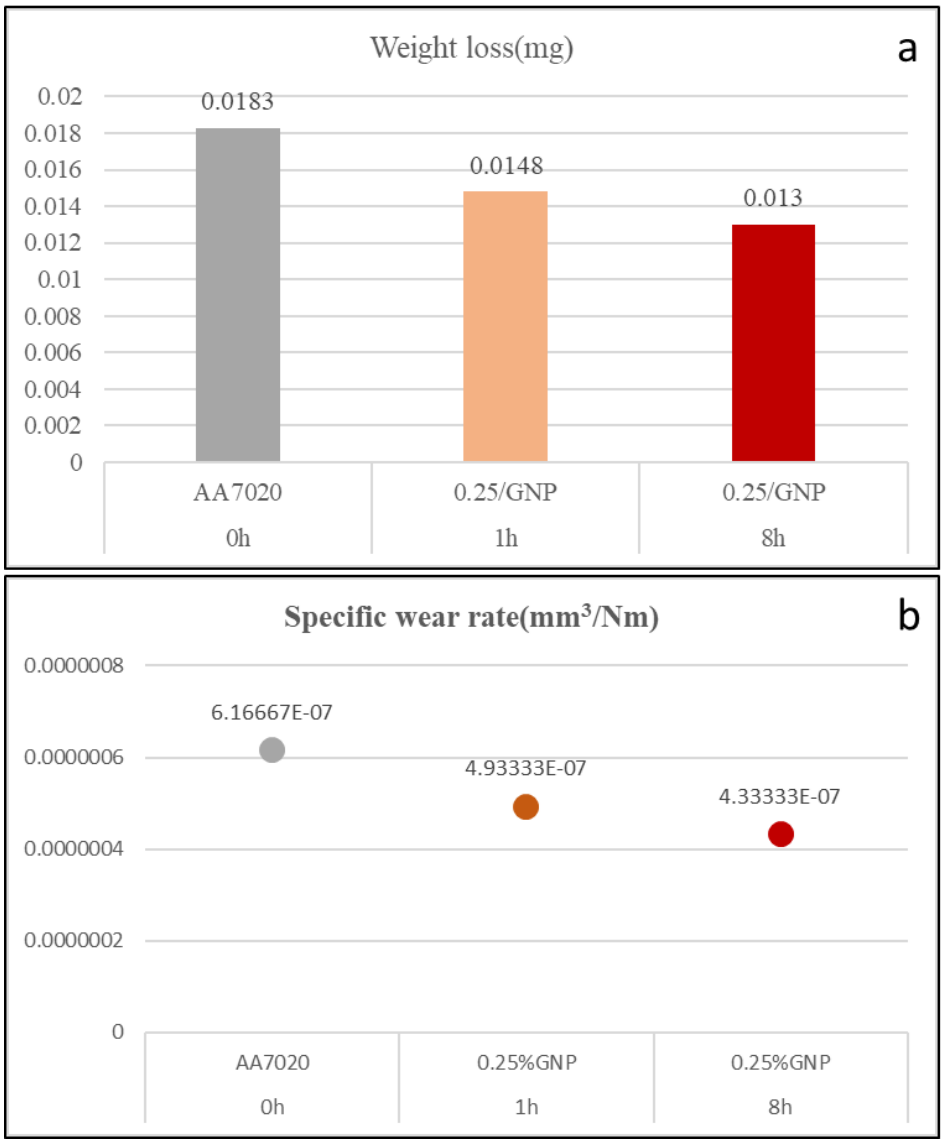

Figure 9. *Weight loss and Specific wear rate*

In wear tests, the resistance to movement between the sample and the abrasive surfaces is known as friction. This resistance is typically defined by the dimensionless coefficient of friction (COF). It is thought that the GNP particles act as lubricants and cause a decrease in the coefficient of friction values depending on the grinding times during the wear test. It is also known that increasing hardness values support this situation. In Figure 10, the highest COF value was determined in the AA7020 sample, while the lowest value was determined as 0.1965 µm in the 8h ground AA7020+10%Fe_3O_4+0.25%GNP sample.

Figure 11 shows the SEM analyses after applying the wear test to the test samples under a 20N load. When the images are examined, deep grooves, debris, plastic deformation, and delamination are detected in the AA7020 alloy without reinforcement and milling. Micro ploughings and plastic deformations increase with the increase in milling time. It is thought that the fact that hybrid reinforcement materials are more complex than the matrix causes the formation of layered regions and deeper grooves. It was observed that the GNP tribe layer was formed, especially in the worn image of the 8h milled sample. This situation was also detected in the SEM/EDS analysis given in Figure 12. The wear behavior of hybrid reinforced composite materials is similar to abrasive wear. The wear behavior of hybrid reinforced materials showed very little difference when applied at different times in the ball milling process.

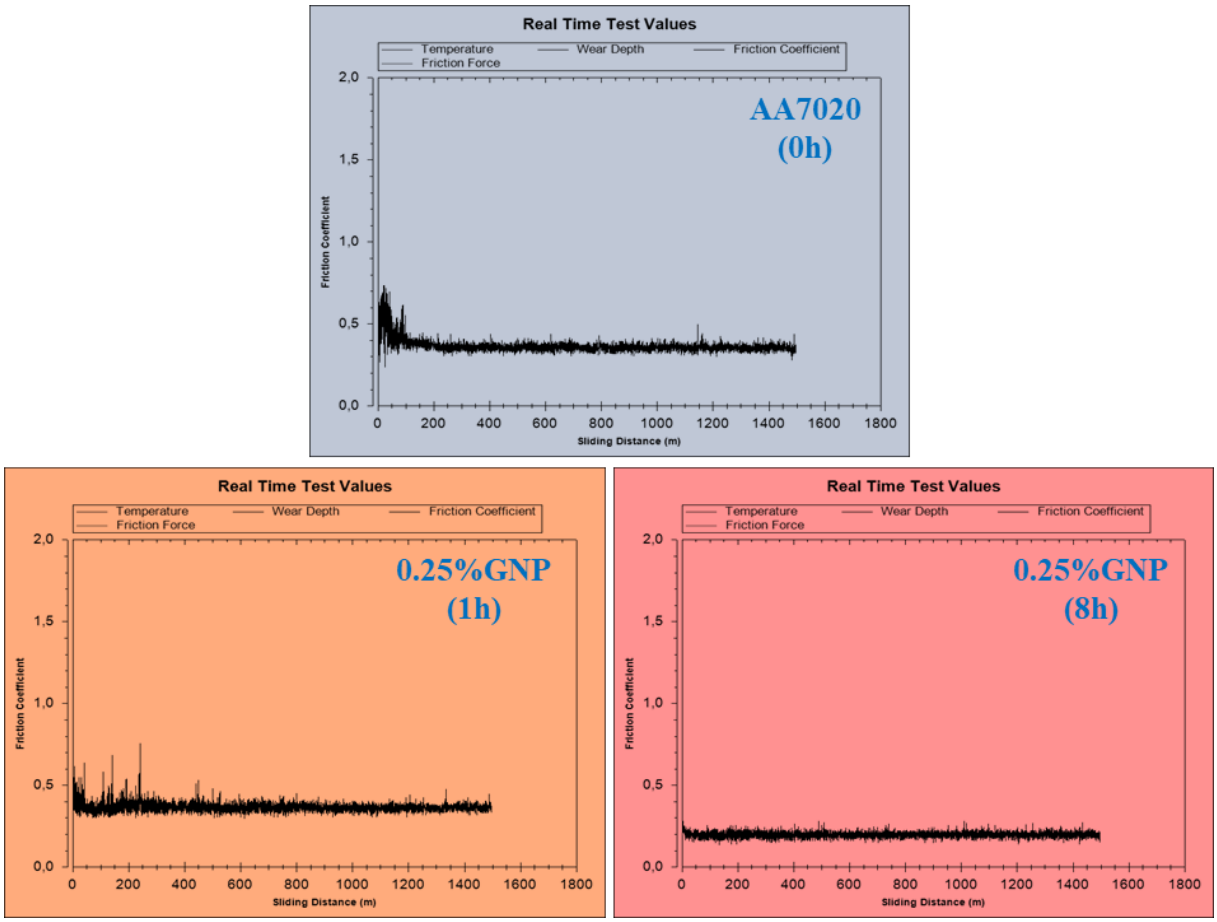

Figure 10. *Coefficient of friction*

In Figure 13, 3D optical profilometer analysis was applied to the test samples after the wear test. When the 3D optical profilometer analyses were examined, it was seen that the AA7020 sample without reinforcement and grinding process was suitable for the wear surface SEM images. It was determined that delamination and regional part breaks occurred mainly. The analysis of hybrid reinforced composite samples determined that the decrease in deep grooves and the increase in plastic deformations with the increase in grinding time affected the surface roughness values. The hardness, COF, and SWR values determined Ra values. While the highest value was determined in the AA7020 alloy without reinforcement (1.077 µm), the lowest value was determined as 0.8886 µm in the 8h milled hybrid reinforced composite sample.

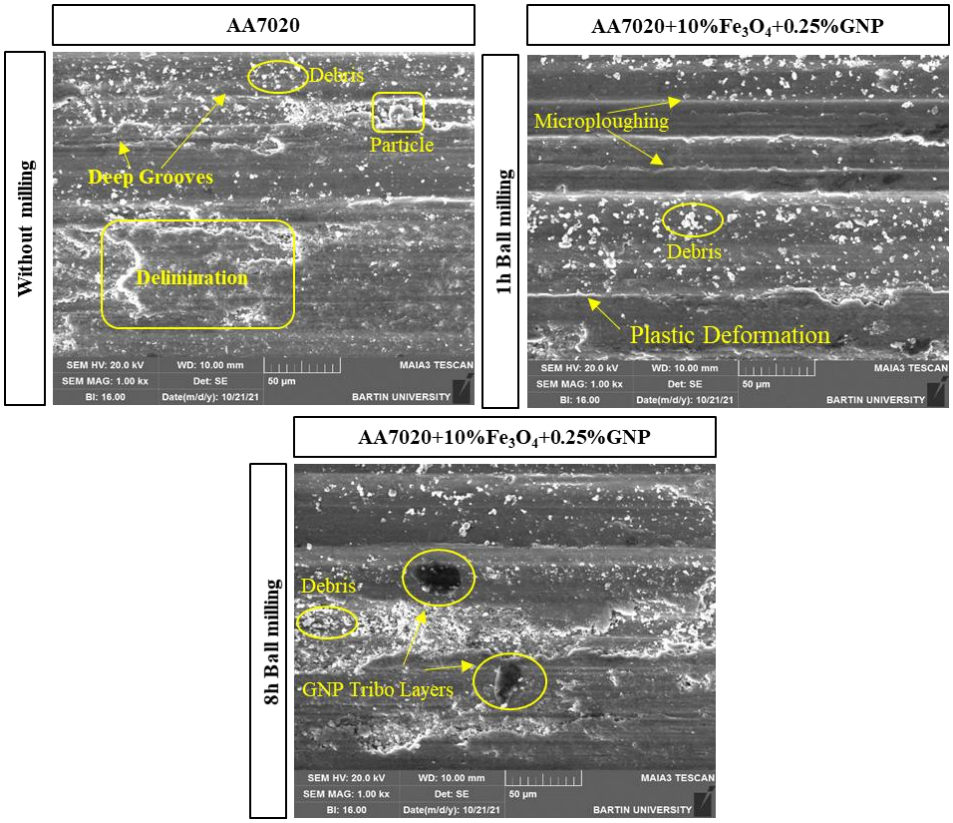

Figure 11. *SEM pictures of the worn surfaces*

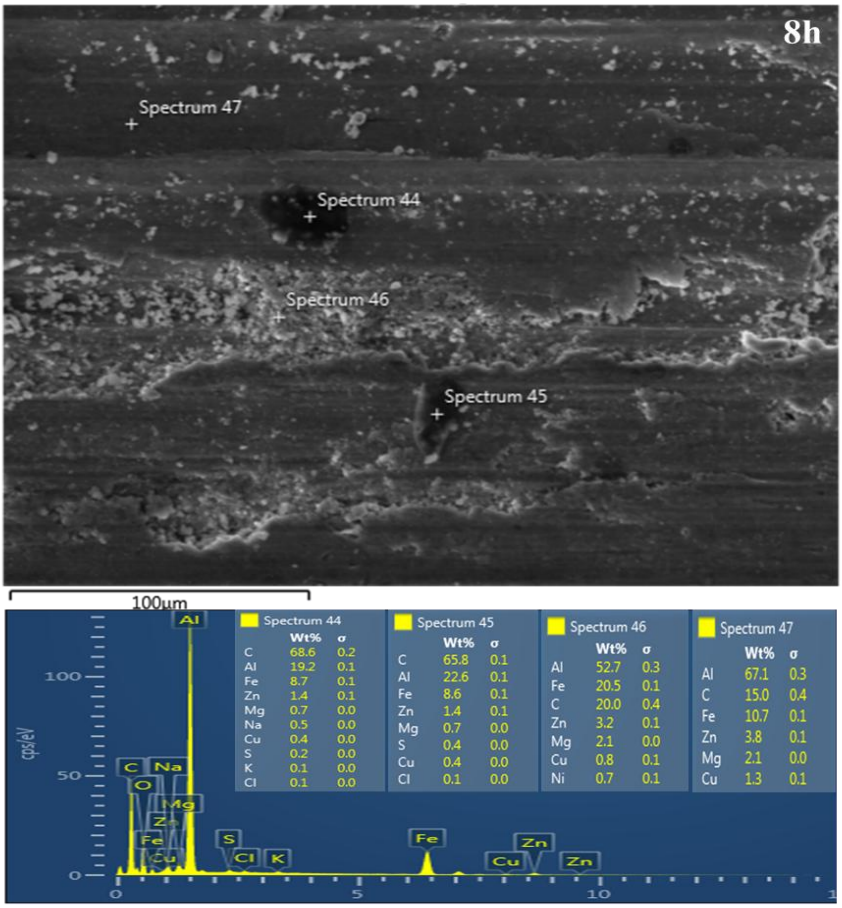

Figure 12. *EDS analysis result images of the worn surface of hybrid composites (8h) material*

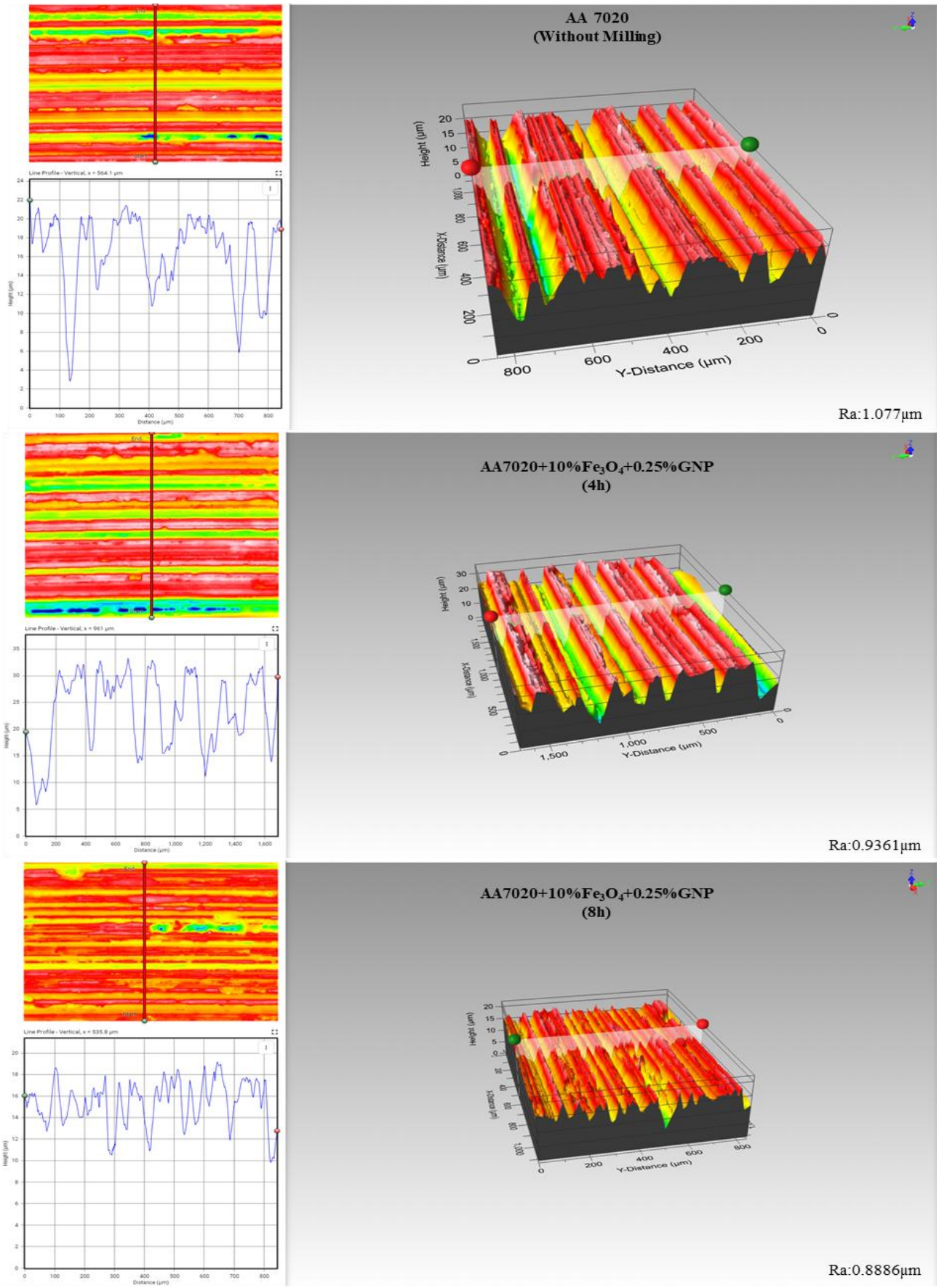

Figure 13. *3D optical profilometer images of the worn surfaces*

4. CONCLUSION

In this study, AA7020 alloy and AA7020+10%Fe_3O_4+0.25%GNP hybrid reinforced composite materials were produced by powder metallurgy hot pressing method. Hybrid-reinforced composite materials were prepared in a ball mixer for 1 and 8 hours. The density, microstructure, hardness, and wear properties of the produced materials were examined. Experimental results are given below.

1. The experimental results revealed a promising trend in the properties of the hybrid-reinforced composite materials. The highest density value, 99.30%, was observed in the 1h milled hybrid reinforced composite material, indicating a significant improvement over the unmilled and non-reinforced AA7020 alloy composite material, which had a density value of 98.8%.

2. The lowest hardness was 109 HV0.5 in unreinforced AA7020 alloy, while the highest hardness value was 118.5 in AA7020+10%Fe_3O_4+0.25%GNP(8h) hybrid reinforced composite material.

3. It was observed that the friction coefficient decreased with increasing grinding time. The highest friction coefficient was determined in the AA7020 alloy material without reinforcement (0.3862 µm). The highest friction coefficient value was determined as 0.1965 µm in the AA7020+10%Fe_3O_4+0.25%GNP(8h) material, decreasing by approximately 50%.

4. It improved the wear resistance and minimized volume losses with increasing grinding time. The lowest specific wear rate was in the AA7020+10%Fe_3O_4+0.25%GNP(8h) hybrid composite (6.16* 10^{-7} mm^3/Nm) material, while the highest specific wear rate was in the AA7020 alloy (4.33* 10^{-6} mm^3/Nm)..

ACKNOWLEDGEMENT

This study was supported by Gazi University BAP with the project number FKB-2023-8950 " Toz Metalurjisi Yöntemiyle Üretilmiş WE43 (Mg-4Y-RE) Matrisli Hibrit Kompozit Malzemelerin Mekanik Özelliklerinin İncelenmesi".

CONFLICT OF INTEREST

The author declares no conflict of interest.

REFERENCES

Jiang, J., Xiao, G., Che, C., & Wang, Y. (2018). Microstructure, mechanical properties and wear behavior of the rheoformed 2024 aluminum matrix composite component reinforced by Al_2O_3 nanoparticles. *Metals*, *8*(6), 460. https://doi.org/10.3390/met8060460

Kanthavel, K., Sumesh, K. R., & Saravanakumar, P. (2016). Study of tribological properties on Al/Al_2O_3/MoS_2 hybrid composite processed by powder metallurgy. *Alexandria Engineering Journal*, *55*(1), 13-17. https://doi.org/10.1016/j.aej.2016.01.024

Karakoç, H., Ovalı, İ., Dündar, S., & Çıtak, R. (2019). Wear and mechanical properties of Al6061/SiC/B_4C hybrid composites produced with powder metallurgy. *Journal of Materials Research and Technology*, *8*(6), 5348-5361. https://doi.org/10.1016/j.jmrt.2019.09.002

Kaya, H., Büyük, U., Çadırlı, E., Şahin, M., & Gündüz, M. (2022). The Effect of Growth Rate on the Microstructure and Mechanical Properties of 7020 Alloys. *Journal of Materials Engineering and Performance*, *31*(2), 1622-1630. https://doi.org/10.1007/s11665-021-06298-8

Kumar, M., Sotirov, N., & Chimani, C. M. (2014). Investigations on warm forming of AW-7020-T6 alloy sheet. *Journal of Materials Processing Technology*, *214*(8), 1769-1776. https://doi.org/10.1016/j.jmatprotec.2014.03.024

Kumar, D., Angra, S., & Singh, S. (2022). Mechanical properties and wear behaviour of stir cast aluminum metal matrix composite: a review. International *Journal of Engineering*, *35*(4), 794-801. https://doi.org/10.5829/ije.2022.35.04A.19

Kumar, D., Angra, S., & Singh, S. (2023). High-temperature dry sliding wear behavior of hybrid aluminum composite reinforced with ceria and graphene nanoparticles. *Engineering Failure Analysis*, *151*, 107426. https://doi.org/10.1016/j.engfailanal.2023.107426

Lakshmikanthan, A., Angadi, S., Malik, V., Saxena, K. K., Prakash, C., Dixit, S., & Mohammed, K. A. (2022). Mechanical and tribological properties of aluminum-based metal-matrix composites. *Materials*, *15*(17), 6111. https://doi.org/10.3390/ma15176111

Michael, A., & John, E. R. (2024). Thermo-Mechanical, Tribological and Microstructural Properties of Aluminium AA8011/B_4C/Graphene Based Hybrid Composites. *Transactions of the Indian Institute of Metals*, *77*(4), 1217-1228. https://doi.org/10.1007/s12666-023-03238-z

Özkan, Z., Gökmeşe, H., & Gökmen, U. (2022). Investigation of the microstructure-hardness and wear performances of hybrid/composite materials Al_2O_3/SiC particle reinforced in AA 7075 matrix. *Science of Sintering*, *54*(2), 177-187. https://doi.org/10.2298/SOS2202177O

Reddy, P. S., Kesavan, R., & Vijaya Ramnath, B. (2018). Investigation of mechanical properties of aluminium 6061-silicon carbide, boron carbide metal matrix composite. *Silicon*, *10*, 495-502. https://doi.org/10.1007/s12633-016-9479-8

Sardar, S., Karmakar, S. K., & Das, D. (2020). Experimental investigation on two-body abrasion of cast aluminum–alumina composites: influence of abrasive size and reinforcement content. *Journal of Tribology*, *142*(3), 031702. https://doi.org/10.1115/1.4045378

Sharma, D. K., Badheka, V., Patel, V., & Upadhyay, G. (2021). Recent developments in hybrid surface metal matrix composites produced by friction stir processing: a review. *Journal of Tribology*, *143*(5), 050801. https://doi.org/10.1115/1.4049590

Srivyas, P. D., Gupta, A., Medhi, T., Arumugam, S., Kumar, D., & Mohan, S. (2023). Corrosion and Tribo-Investigations on Alumina–Graphene-Doped Hybrid Aluminium Composites. *Transactions of the Indian Institute of Metals*, *76*(12), 3281-3291. https://doi.org/10.1007/s12666-023-02999-x

Taşcı, U., & Bostan, B. (2022). Investigation of microstructure and tribological behavior of WE43/nano B_4C composites produced by spark Plasma sintering. *Gazi University Journal of Science Part A: Engineering and Innovation*, *9*(4), 562-569. https://doi.org/10.54287/gujsa.1214668

Taşcı, U., Yılmaz, T. A., Karakoç, H., & Karabulut, Ş. (2024). Enhancing Wear Resistance and Mechanical Behaviors of AA7020 Alloys Using Hybrid Fe_3O_4-GNP Reinforcement. *Lubricants*, *12*(6), 215. https://doi.org/10.3390/lubricants12060215

Zheng, K., Du, X., Qi, H., Zhao, T., Liu, F., & Sun, B. (2020). Sliding-Wear Behavior of Aluminum-Matrix Composites Reinforced with Graphene and SiC Nanoparticles. *Materials and Technology*, *54*(1). https://doi.org/10.17222/mit.2019.104